SAE TECHNICAL PAPER SERIES

1999-01-1065

Development of an Improved Airbag-Induced Thermal Skin Burn Model

Matthew P. Reed, Jonathan D. Rupp, Steven J. Reed and Lawrence W. Schneider
University of Michigan Transportation Research Institute

Reprinted From: Air Bag Technology 1999 (SP-1411)

SAE The Engineering Society For Advancing Mobility Land Sea Air and Space® INTERNATIONAL

**International Congress and Exposition
Detroit, Michigan
March 1-4, 1999**

400 Commonwealth Drive, Warrendale, PA 15096-0001 U.S.A. Tel: (724) 776-4841 Fax: (724) 776-5760

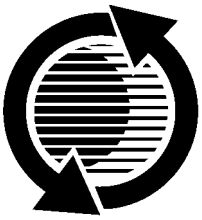

ISSN 0148-7191

Printed in USA

1999-01-1065

Development of an Improved Airbag-Induced Thermal Skin Burn Model

Matthew P. Reed, Jonathan D. Rupp, Steven J. Reed and Lawrence W. Schneider
University of Michigan Transportation Research Institute

ABSTRACT

The UMTRI Airbag Skin Burn Model has been improved through laboratory testing and the implementation of a more flexible heat transfer model. A new impinging jet module based on laboratory measurements of heat flux due to high-velocity gas jets has been added, along with an implicit finite-difference skin conduction module. The new model can be used with airbag gas dynamics simulation outputs, or with heat flux data measured in the laboratory, to predict the potential for thermal skin burn due to exposure to airbag exhaust gas.

INTRODUCTION

Most contemporary automobile airbags are inflated by the rapid combustion of a propellant that produces high-temperature gas. High gas temperatures allow the required internal airbag pressure to be obtained with less gas mass than would be necessary at lower temperatures, but also may increase the potential for thermal burn to occupants exposed to the gas. Thermal burns due to airbag exhaust gas exposure have been reported in field deployments (1, 2[1]). Reinfurt et al. (3) estimated that approximately 7 percent of drivers who experienced a steering-wheel airbag deployment reported a thermal burn. Recent trends in airbag design have led to smaller inflators and hotter inflation gases, increasing the interest in accurate methods for assessing airbag thermal burn potential.

Laboratory investigations and modeling have been conducted to address airbag thermal burn issues. Reed et al. (4) determined the sensitivity of human skin to high-velocity, high-temperature gas exposures and used the data to validate a mathematical model of airbag-induced skin burn. The original UMTRI Airbag Skin Burn Model (ASBM) included airbag inflation simulation and skin burn simulation modules. A FORTRAN version of the model was developed for general application, and included a simple occupant interaction simulation (5). Although a number of other burn injury models have been developed (6-9), including a model of heat transfer to the skin due to airbag gas flows (10), the UMTRI ASBM remains the only model that has been validated using convection burn threshold data from human subjects.

While effective for some types of simulations, the original model had some important limitations, particularly in the heat transfer module. Heat conduction in the skin was modeled using efficient, closed-form solutions, but this approach necessitated a number of simplifying assumptions that reduced the generality and accuracy of the simulations. Boundary conditions at the skin surface were assumed to be constant during airbag exhaust gas flow, and the effects of depth-varying thermal properties in the skin were not addressed. The model also relied on algorithms for calculating the heat transfer to the skin due to impinging hot gas that were found in laboratory testing to be inadequate.

A new model has now been developed that overcomes many of the limitations of the previous model, and provides substantial new capabilities that allow the model to be used both with mathematical airbag simulation outputs and with thermal measurement data from laboratory tests. The new UMTRI Airbag Skin Burn Model (ASBM) gives accurate predictions of burn risk for a wide range of high-temperature, high-velocity gas jet exposures that may result from occupant interaction with an airbag.

MODEL STRUCTURE

Figure 1 shows a schematic of the ASBM. The airbag inflation gas-dynamics simulation that was part of the original model has been dropped, since most potential ASBM users have other, more sophisticated simulation capability. Instead, the ASBM is designed to work with output data from other simulation software. The model consists of three modules. The impinging gas jet model calculates the heat transfer to the skin that results from gas flow through a discrete airbag vent onto the skin. The

1. Numbers in parentheses denote references at the end of the paper.

heat transfer module simulates heat conduction into and through the skin, and the burn injury module calculates the potential for thermal burn as a function of the temperature history in the skin.

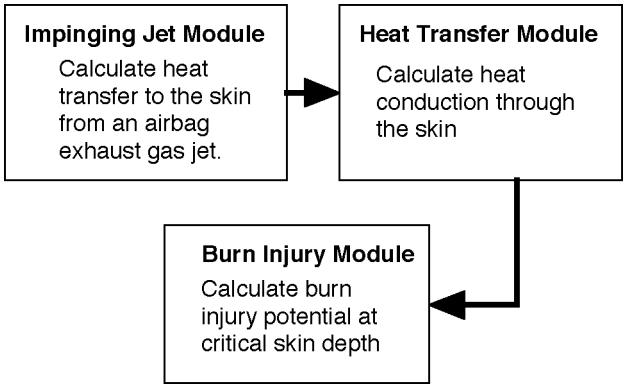

Figure 1. UMTRI Airbag Skin Burn Model schematic.

IMPINGING JET MODULE – One of the important advancements in the model is the development of entirely new mathematical models to calculate the heat flux to the skin that results from an impinging gas jet. The corresponding models in the original ASBM were adapted from empirical relationships in the heat transfer literature (11). Testing at UMTRI with airbags and gas jet simulators demonstrated that these models did not accurately reflect the effects of gas jet diameter and distance on heat transfer.

A research program was conducted to develop a new impinging jet model. A laboratory gas jet simulator, or heatgun, was used to create gas jets with a wide range of gas speed and temperature. Jet diameter was varied between 5 and 20 mm, and the distance between the jet outlet and the target surface varied from 0.5 to 10 times the jet diameter. The heat transfer to the target surface was measured with a commercial heat flux meter manufactured by Vatell, Inc. The 4-mm-diameter sensor produces a signal proportional to heat flux, and a surface temperature sensor allows the flux reading to be interpreted in terms of heat transfer coefficient.

Data from this testing were used to create a mathematical model that calculates the surface heat transfer coefficient resulting when an airbag exhaust gas jet impinges on the skin. The model takes as input the airbag exhaust gas velocity and temperature as a function of time, along with the gas thermal properties and the exhaust vent geometry.

HEAT TRANSFER MODULE – Heat transfer into the skin is simulated by a one-dimensional, finite-difference conduction model. Figure 2 illustrates the model schematically. The skin is represented by a series of discrete nodes, beginning with the skin surface and extending 1 mm into the skin. The Fourier conduction equation,

$$\frac{\partial^2 T}{\partial x^2} = \frac{1}{\alpha_s}\frac{\partial T}{\partial t} \qquad (1)$$

is discretized to express the temperature of each node as a function of the temperatures at the adjacent nodes (12, 13). The complete mathematical formulation of the model is presented in the Appendix. A fully implicit solution method is implemented that is unconditionally stable for a wide range of node spacings and time steps. The model proceeds by a marching solution, solving for the temperature at each node at each of many small time steps (typically 1 ms).

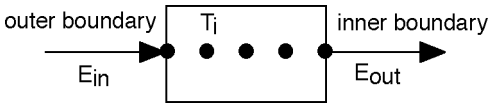

Figure 2. Schematic illustration of the finite-difference heat transfer module (actual number of nodes is typically ≥100).

The finite-difference solution has several advantages over the previously used closed-form solution. The thermal properties may be varied with depth, to account for the varying thermal conductivity and heat capacity of the epidermis and dermis. The surface boundary conditions may vary with time to simulate transient changes in the airbag exhaust gas temperature and velocity. Further, time-varying surface flux data, such as those obtained in laboratory testing with airbags, may be input to the model.

The heat transfer model has been numerically validated using four techniques. First, closed-form solutions are available to describe one-dimensional heat transfer into a semi-infinite solid initially at a constant temperature (12). Using a large number of nodes, the new heat transfer module matches the solutions given by the closed-form equations for convection, flux, and prescribed-surface-temperature boundary conditions. Second, the depth-varying thermal properties were validated by running a model with two different thermal layers, each described by 10 nodes, for a large number of time steps. The resulting temperature profile showed the expected linear profiles within each material, with slopes corresponding to the specified thermal conductivity. Third, the energy balance in the model was evaluated for each of the previously described simulations. The energy change within the model accurately reflected the energy input to the model for long-duration simulations, indicating minimal compounding of numerical errors. Lastly, the effectiveness of the time-varying surface condition simulations was evaluated by comparing the model results to those obtained using the finite Fourier-series approximation solution used in the previous model (4) for an input consisting of a series of steps in the surface convection coefficient. Again, good agreement was obtained.

BURN INJURY MODULE – The burn injury module is based on the omega burn function originally developed by Henrique and Moritz (6), and widely used in burn injury research (4-9). As in the original ASBM, burn injury is modeled as a rate-dependent process that proceeds

more quickly as the tissue temperature increases. The burn injury parameter, Ω, is calculated as a function of the temperature history at the selected tissue depth,

$$W = G \int_0^t Exp\left[\frac{-\Delta E}{R\,T(t)}\right] dt \qquad (2)$$

where T(t) is the temperature versus time at the selected skin depth, R is the ideal gas constant (8.3144 J/g-mol/K), and ΔE and G are constants determined by fitting to injury data. The skin depth chosen is usually the depth of the basal epidermal layer, which is the most superficial layer in which thermal injury can induce necrosis. A typical value for the critical skin depth is 80 μm (4). The values of ΔE and G are chosen so that the value of omega is one at the threshold for a second-degree burn.

A wide range of ΔE and G values have been used in previous research (4-9). For the current version of the UMTRI ASBM, new constants were calculated based on the human burn tolerance data for gas-jet exposures reported by Reed et al. (4). In previous testing (4), human volunteers were exposed to 10-mm-diameter air jets at temperatures ranging from 350 to 550 °C and velocities ranging from 51 to 91 m/s. At fourteen different temperature/velocity conditions, the exposure duration was varied in 10-ms increments to determine the exposure duration corresponding to the threshold for second-degree burn. These data form the primary basis for tuning the ASBM.

IMPLEMENTATION AND APPLICATION

The ASBM is written in ANSI C and can be compiled to run in most computer environments. Data inputs to the model are in the form of ASCII (text) files with a prescribed format. Airbag exhaust gas temperature and velocity data, or surface flux data from laboratory measurements, can be input in tabular format. The model is implemented as a general purpose heat transfer solver, so that a variety of conduction, convection, and flux boundary conditions can be input, as well as any desired material properties. However, the default settings simulate heat transfer to a two-layer, one-mm-thick skin model, comprised of 80 μm of epidermis with 920 μm of dermis. Different thermal properties are used for the two layers (4-7). The temperature of the interior node is maintained at body temperature, while a convection or flux condition is imposed at the surface (see Appendix).

The primary application of the ASBM is to assess the burn potential of prototype airbag systems. The effects of changes in exhaust gas velocity and temperature on burn potential can be assessed, as well as the influence of exhaust vent diameter and the distance between the vent and the skin surface. To use the model early in the development cycle, outputs from an airbag deployment simulation model are input to the ASBM. The model results can indicate whether a thermal burn would be likely if the airbag exhaust gas impinged on an occupant's skin. The surface conditions input to the model include the conditions of hot-gas flow during the airbag deployment and the ambient cooling that follows. After a prototype module has been developed, the thermal flux produced by the airbag exhaust gas jet can be measured in a laboratory deployment. The flux data can be input to the model to obtain another assessment of burn potential.

RESULTS

The ASBM was exercised to predict temperature histories at the basal epidermal depth for each of these temperature/velocity conditions for which human subject burn threshold data are available. A numerical optimization procedure was used to calculate ΔE and G values with omega set equal to one for each of the temperature histories. Since many combinations of ΔE and G can produce omega equal to one for a particular temperature history, ΔE was set to 623580 J/mol, the value used in the original ASBM. The new value of G that best fits the human convection-burn data is 3.44×10^{94} (dimensionless). Figure 3 demonstrates the ability of the model to predict thermal burn thresholds for short-duration convection exposures. The correlation between the predicted and observed burn thresholds is 0.90, compared with 0.88 for the previous model (4).

The new model produces essentially the same performance as the old model for predicting this set of human subject burn threshold data. However, the new impinging jet module and the finite-difference heat transfer module allow the new ASBM to be used with time-varying thermal inputs typical of actual airbag exposures.

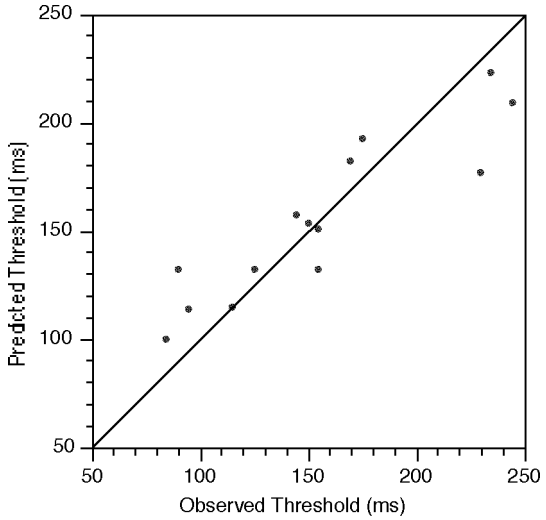

Figure 3. Predicted second-degree-burn exposure duration thresholds for a range of high-temperature, high-velocity gas jet exposures compared with 14 observed human burn thresholds (r = 0.90).

DISCUSSION

The new UMTRI Airbag Skin Burn Model improves on the functionality of the original model and provides additional flexibility. A new impinging jet heat transfer module is used to calculate the heat transfer to the skin. The finite-difference model of heat transfer in the skin allows time-varying boundary conditions to replicate airbag deployment scenarios more completely, and the burn injury assessment algorithm has been retuned to match human burn sensitivity data.

Work to improve the model further is proceeding in three areas:

- Preliminary measurements of the heat flux due to gas flow through porous fabric indicate that, under certain conditions, thermal burns could result. Further research will be necessary to develop the capability to predict burn risk for flows through fabric.
- Most of the research to date has been conducted with nitrogen or air. Although the models are configured such that the results should be accurate for any dry gas, the ASBM will not accurately predict the burn risk associated with gases with substantial water vapor content. Additional study of the influence of water vapor on these heat transfer modes is needed.
- In addition to convection burns, direct skin exposures to hot airbag and module surfaces may also pose a burn risk. Investigations of contact burn scenarios leading to the implementation of contact burn simulations in the ASBM are underway.

CONCLUSIONS

The UMTRI ASBM provides the capability to include burn potential assessment in the airbag design process. Further improvements to the model will improve generality of the applications, and may lead to more comprehensive assessments.

ACKNOWLEDGMENTS

The model described in this paper was developed and improved over several years with support from a number of sources, including contributions from Autoliv, Delphi, Honda Research and Development, Nissan, and TRW. Most recently, all five of these companies have participated in the UMTRI Airbag Skin Burn Affiliates program, an industry group that supports airbag research at UMTRI.

REFERENCES

1. Hallock, G.G. (1997). Mechanisms of burn injury secondary to airbag deployment. *Annals of Plastic Surgery*, 39:111-113.
2. Antosia, R.E., Partridge, R.A., and Virk, A.S. (1995). Air bag safety. *Annals of Emergency Medicin*e, 25:794-798.
3. Reinfurt, D.W., Green, A.W., Campbell, B.J., and Williams, A.F. (1993). *Survey of attitudes of drivers in air bag deployment crashes.* Technical Report. Insurance Institute for Highway Safety, Arlington, VA.
4. Reed, M.P., Schneider, L.W., and Burney, R.E. (1994). Laboratory investigations and mathematical modeling of airbag-induced skin burns. Technical Paper No. 942217. *Proc. 38th Stapp Car Crash Conference*, pp. 177-190. Society of Automotive Engineers, Warrendale, PA.
5. Bowman, B.M. and Reed, M.P. (1996). *User's Guide for the UMTRI Airbag Skin Burn Model.* Technical Report UMTRI-96-5. University of Michigan Transportation Research Institute, Ann Arbor, MI.
6. Henrique, F.C. and Moritz, A.R. (1947). Studies of thermal injury. I. The conduction of heat to and through the skin and the temperatures attained therein. *American Journal of Pathology*, 23:531-549.
7. Weaver, J.A. and Stoll, A.M. (1969). Mathematical model of skin exposed to thermal radiation. *Aerospace Medicine*, 40(1):24-30.
8. Torvi, D.A. and Dale, J.D. (1994). Finite element model of skin subjected to a flash fire. *Journal of Biomechanical Engineering*, 116(3):250-255
9. Bamford, G.J. and Bodell, W. (1995). ICARUS: a code for evaluating burn injuries. *Fire Technology*, 31(4):307-335.
10. Thomas, S.K. and Eilers, G.J. (1996). Numerical and analytical modeling of heat transfer into the skin due to airbag deployment. *Proc. 1996 ASME National Heat Transfer Conference*, Part 2. American Society of Mechanical Engineers, New York.
11. Martin, H. (1977). Heat and mass transfer between impinging gas jets and solid surfaces. *Advances in Heat Transfer*, 13:1-60.
12. Incropera, F.P. and Dewitt, D.P. (1985). *Introduction to Heat Transfer.* Wiley, New York.
13. Pantakar, S.V. (1980). *Numerical Heat Transfer and Fluid Flow.* McGraw-Hill, New York.

APPENDIX

FINITE DIFFERENCE CONDUCTION MODEL FORMULATION

The skin conduction model in the UMTRI ASBM is based on a generic, one-dimensional heat transfer solution for a finite slab. This Appendix describes the formulation of the mathematical model.

GENERAL FINITE DIFFERENCE METHODOLOGY – For implicit finite-difference equations, the temperature at each node throughout the depth of the material is described by an equation that is a function of the material properties, the known current temperature at the node, and the unknown temperature at time p+1 of the node and surrounding nodes. If the equations for the temperatures of the nodes are written in matrix form, the resulting matrix will be tridiagonal and have the following form:

$$[A][T] = [C]$$

For five nodes, the model schematic is as follows:

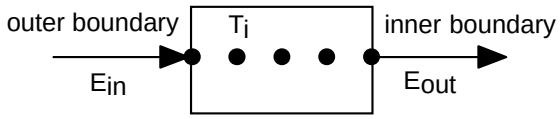

and the node equations may be written:

$$[A] = \begin{vmatrix} OuterBC1 & OuterBC2 & 0 & 0 & 0 \\ a & b & c & 0 & 0 \\ 0 & a & b & c & 0 \\ 0 & 0 & a & b & c \\ 0 & 0 & 0 & InnerBC1 & InnerBC2 \end{vmatrix}$$

$$[T] = \begin{vmatrix} T_0 \\ T_1 \\ T_2 \\ T_3 \\ T_4 \end{vmatrix}^{p+1} \qquad [C] = \begin{vmatrix} T_0 + outer\ BC\ info \\ T_1 \\ T_2 \\ T_3 \\ T_4 + inner\ BC\ info \end{vmatrix}^{p}$$

where

a, b, c, OuterBC , *InnerBC* , *inner BC info*, and *outer BC info* are described by the appropriate node temperature formulations shown below (see also Table 1). Each of the T_i corresponds to the temperature at the specified node, with the left-most (outer) node numbered zero. The superscript *p* refers to the previous time step, and *p+1* refers to the next (solution) time step.

To solve for [T], the equation is rewritten in the form:

$$[A]^{-1}[C]=[T]$$

For tridiagonal matrices, solution methods are available that are linear in the number of nodes, eliminating the need to invert large matrices.

DERIVATION OF THE FINITE-DIFFERENCE SKIN HEAT TRANSFER MODEL

The finite difference equations were obtained by performing energy balances about the three areas of interest: the outer surface, the interior, and the inner surface. The outer surface represents the external epidermis (skin surface), the interior consists of the dermis and epidermis, and the inner surface represents conditions that occur at a user specified depth within the dermis.

For each surface, three alternative boundary conditions were modeled: a convective boundary condition, a conductive boundary condition (flux at a the surface), and a constant surface temperature condition. For the interior nodes, only conduction with no internal heat generation is required.

Definition of Variables:

q”	surface thermal flux (W/m^2)
h	convection coefficient (W/m^2/K)
A	area (m^2)
T_∞	ambient temperature (K)
T_i^p	temperature at node i and time p. (K)
Bi	Biot Number (h Δx /k)
x	depth (m)
k	thermal conductivity at node i (W/m/K)
ρ	density of skin at node i (kg/m^3)
C_p	specific heat capacity (J/kg)
t	time (second)
α	thermal diffusivity (k/ (ρ Cp))
Fo	Fourier Number (α Δt/(Δx^2))

DERIVATION OF THE INTERIOR NODE EQUATIONS

$$\dot{E}_{in} - \dot{E}_{out} = \dot{E}_{stored}$$

$$\frac{k^* A}{\Delta x}(T_{i-1}^{p+1} - T_i^{p+1}) + \frac{k^* A}{\Delta x}(T_{i+1}^{p+1} - T_i^{p+1}) = \rho_i Cp_i A \frac{\Delta x}{2\Delta t}(T_i^{p+1} - T_i^p)$$

k^* is an average thermal conductivity between the node 0 and 1 (see reference 13)

$$k^* = \frac{2k_0}{k_0 + k_1}$$

rearranging :

$$-\frac{2k_{i-1}}{k_i + k_{i-1}} Fo_i T_{i-1}^{p+1} + \left(1 + 2\left(\frac{k_{i-1}}{k_i + k_{i-1}} + \frac{k_{i+1}}{k_i + k_{i+1}}\right) Fo_i\right) T_i^{p+1} - \frac{2k_{i+1}}{k_i + k_{i+1}} Fo_i T_{i+1}^{p+1} = T_i^p$$

DERIVATION OF THE CONVECTIVE BOUNDARY CONDITION FOR THE OUTER SURFACE

$$\dot{E}_{in} - \dot{E}_{out} = \dot{E}_{stored}$$

$$hA(T_\infty^p - T_o^p) + \frac{k^* A}{\Delta x}(T_1^{p+1} - T_0^{p+1}) =$$

$$\rho_0 Cp_0 A \frac{\Delta x}{2\Delta t}(T_0^{p+1} - T_0^p)$$

rearranging:

$$(1 + \frac{4k_1}{k_0 + k_1} Fo_0 + 2Bi_0 Fo_0)T_0^{p+1} - \frac{4k_1}{k_0 + k_1} Fo_0 T_1^{p+1} =$$

$$T_0^p + 2Bi_0 Fo_0 T_\infty^p$$

DERIVATION OF THE CONDUCTIVE BOUNDARY CONDITION FOR THE OUTER SURFACE

$$\dot{E}_{in} - \dot{E}_{out} = \dot{E}_{stored}$$

$$q''^p A + \frac{k^* A}{\Delta x}(T_1^{p+1} - T_0^{p+1}) = \rho_0 Cp_0 A \frac{\Delta x}{2\Delta t}(T_0^{p+1} - T_0^p)$$

rearranging:

$$(1 + \frac{4k_1}{k_0 + k_1} Fo_0)T_0^{p+1} - \frac{4k_1}{k_0 + k_1} Fo_0 T_1^{p+1} = T_0^p - 2q''^p \frac{\Delta t}{\Delta x}\frac{\alpha_0}{k_0}$$

DERIVATION OF SURFACE TEMPERATURE BOUNDARY CONDITIONS – The surface temperature boundary conditions require no derivation since it consists of setting $T_{surface}$ (either outer or inner) to be equal to a specified values, i.e.,

$$T_{inner}^p = T_{surface,inner}(t), \;\; T_{outer}^p = T_{surface,outer}(t)$$

DERIVATION OF CONVECTIVE INNER BOUNDARY CONDITION – Derivation of the convective inner boundary condition is essentially identical to the derivation of the convective outer boundary condition. The differences all result from changes in sign.

$$-\frac{4k_{i-1}}{k_{i-1} + k_i} Fo_i T_{i-1}^{p+1} + (1 + \frac{4k_{i-1}}{k_i + k_{i-1}} Fo_i + 2Bi_i Fo_i)T_i^{p+1} = T_i^p + 2Bi_i Fo_i T_\infty^p$$

DERIVATION OF CONDUCTIVE INNER BOUNDARY CONDITION – Derivation of the conductive inner boundary condition is essentially identical to the derivation of the conductive outer boundary condition. The differences result from changes in sign (i.e., q'' is positive in the direction of increasing depth).

$$-\frac{4k_{i-1}}{k_{i-1} + k_i} Fo_i T_{i-1}^{p+1} + (1 + \frac{4k_{i-1}}{k_{i-1} + k_i} Fo_i)T_i^{p+1} = T_i^p - 2q''^p \frac{\Delta t}{\Delta x}\frac{\alpha_i}{k_i}$$

Tables 1 and 2, below, define each of the expressions in the A matrix according to the preceding derivations

Table 1. Boundary Condition Expressions

	Convective	**Conductive**	**Contact**
OuterBC1	$1 + \frac{4k_1}{k_0 + k_1} Fo_0 + 2Bi_0 Fo_0$	$1 + \frac{4k_1}{k_0 + k_1} Fo_0$	1
OuterBC2	$-\frac{4k_1}{k_0 + k_1} Fo_0$	$-\frac{4k_1}{k_0 + k_1} Fo_0$	0
Outer BC info	$2Bi_0 Fo_0$	$-2q''^p \frac{\Delta t}{\Delta x}\frac{\alpha_0}{k_0}$	0
InnerBC1	$-\frac{4k_{i-1}}{k_{i-1} + k_i} Fo_i$	$-\frac{4k_{i-1}}{k_{i-1} + k_i} Fo_i$	0
InnerBC2	$1 + \frac{4k_{i-1}}{k_i + k_{i-1}} Fo_i + 2Bi_i Fo_i$	$1 + \frac{4k_{i-1}}{k_{i-1} + k_i} Fo_i$	1
Inner BC info	$2Bi_i Fo_i$	$-2q''^p \frac{\Delta t}{\Delta x}\frac{\alpha_i}{k_i}$	0

Table 2. Interior Node Expressions

Symbol	Expression
a	$-\frac{2k_{i-1}}{k_i + k_{i-1}} Fo_i$
b	$1 + 2\left(\frac{k_{i-1}}{k_i + k_{i-1}} + \frac{k_{i+1}}{k_i + k_{i+1}}\right) Fo_i$
c	$-\frac{2k_{i+1}}{k_i + k_{i+1}} Fo_i$